ICES Journal of
Marine Science

ICES CIEM International Council for the Exploration of the Sea Conseil International pour l'Exploration de la Mer

ICES Journal of Marine Science (2016), 73(8), 1987–1997. doi:10.1093/icesjms/fsw084

Contribution to the Symposium: '*Marine Acoustics Symposium*'

Original Article

A method for controlled target strength measurements of pelagic fish, with application to European anchovy (*Engraulis encrasicolus*)

Mathieu Doray[1,*], Laurent Berger[2], Naig Le Bouffant[2], Jean Yves Coail[3], Jean Philippe Vacherot[4], Xavier de La Bernardie[5], Pierre Morinière[6], Elisabeth Lys[5], Romain Schwab[2], and Pierre Petitgas[1]

[1]*Unité Écologie et Modèles pour l'Halieutique, Ifremer Nantes, Rue de l'Ile d'Yeu, BP 21105, 44300 Nantes Cedex 3, France*
[2]*Service Acoustique Sous-marine et Traitement de l'Information, Ifremer Brest, Brest, France*
[3]*Service Ingénierie et Instrumentation Marine, Ifremer Brest, Brest, France*
[4]*Laboratoire de Technologie et de Biologie Halieutique, Ifremer Lorient, Lorient, France*
[5]*UMR SUBATECH, CNRS (IN2P3) - École des Mines de Nantes - Université de Nantes, Nantes, France*
[6]*Aquarium La Rochelle, La Rochelle, France*

**Corresponding author: tel: + 33 (0)2 40 37 41 65; fax: + 33 (0)2 40 37 40 75; e-mail: mathieu.doray@ifremer.fr.*

Doray, M., Berger, L., Bouffant, N. L., Coail, J. Y., Vacherot, J. P., de La Bernardie, X., Morinière, P., Lys, E., Schwab, R., and Petitgas, P. 2016. A method for controlled target strength measurements of pelagic fish, with application to European anchovy (*Engraulis encrasicolus*). – ICES Journal of Marine Science, 73: 1987–1997.

Received 27 August 2015; revised 7 April 2016; accepted 7 April 2016; advance access publication 19 July 2016.

Measuring fish target strength (TS) in the wild is challenging because: (i) TS varies versus physical (orientation relative to the incident sound wave, size, and depth) and physiological fish attributes (maturity and condition), (ii) the target species and its aforementioned attributes are difficult to assess in near real time, and (iii) in the case of packed fish schools, accepted echoes may originate from multiple unresolved targets. We propose a method for controlled TS measurements of densely packed small pelagic fish during daytime, based on the joint use of a Remotely Operated Towed Vehicle, "EROC", with a pelagic trawl fitted with a codend opening system, "ENROL". EROC, equipped with a 70-kHz split-beam echosounder (Simrad EK60) and a low-light black and white camera, can be moved inside the fishing trawl. Pelagic fish are funnelled into the open trawl and their TS is measured in the middle of the net, where small groups actively swim towards the trawl mouth. The swimming behaviour allows for near-dorsal TS to be measured, minimizing the large effect of incidence angle on TS variability. The EROC camera, located near the open codend, provides optical identification of the species. This method was used to measure the TS of European Anchovy, *Engraulis encrasicolus* in the Bay of Biscay during 2014. The mean, near dorsal TS was −43.3 dB, for a mean fork length of 12.5 cm. This value is compared to published values of clupeiforms mean TS obtained for a range of natural incidence angles and discussed in the light of TS modelling results obtained for *E. encrasicolus*.

Keywords: acoustics, deformed cylinder model, *Engraulis encrasicolus*, remotely operated vehicle, target strength, video.

Introduction

Knowledge of target strength (TS) of single fish is important for acoustic target classification (Barange, 1994; Doray *et al.*, 2006), and abundance estimation (Rose, 1992; Jech and Horne, 2001). However, measuring fish TS in the wild is challenging because: (i) TS largely varies versus physical (orientation relative to the incident sound wave, size, and depth) and physiological fish attributes (Horne, 2000), (ii) the target species and its aforementioned attributes are difficult to assess at the same time as acoustic measurements (Simmonds and MacLennan, 2005), and (iii) multiple

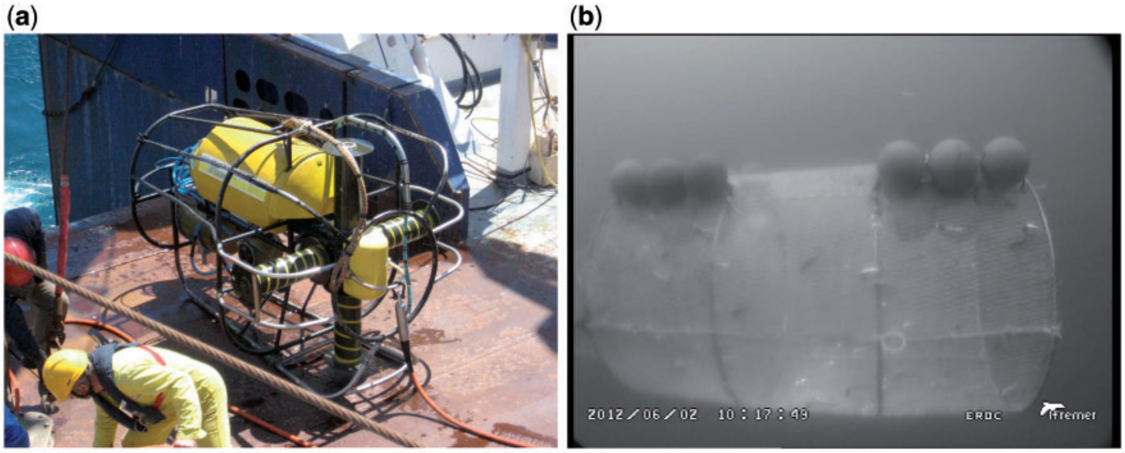

Figure 1. (a) Remotely Operated Towed Vehicle EROC and (b) underwater picture of the open codend ENROL taken by the EROC camera.

targets echoes can be accepted as single target ones in the case densely packed fish schools (Soule *et al.*, 1995). Acoustic-Optic Systems (AOS) combining scientific echosounders and camera have been successfully used to record TS of loosely aggregated fish, while observing species (Doray *et al.*, 2007; Ryan *et al.*, 2009; O'Driscoll *et al.*, 2013), and, using a stereo camera, observing species, size, and orientation (Kubilius and Ona, 2012).

During daytime, small pelagic fish congregate in schools that are too densely packed to resolve individual targets with hull-mounted echosounders (Sawada *et al.*, 2009). At night, small pelagic fish schools often disperse and migrate near to the surface (Fréon and Misund, 1999) where they cannot be detected by down-projecting hull-mounted echosounders. Moreover, at night, small pelagic fish usually mix with other scatterers. Despite these potential complications, TS measurements have been made at night using hull-mounted echosounders (Foote, 1987; Barange *et al.*, 1996; Peltonen and Balk, 2005; Zhao *et al.*, 2008), but in these cases, the fish in the study areas were dominated by the target species.

In these studies, the distribution of fish orientation relative to the incident sound wave is assumed to represent the average incident angle for all measures of the population (Simmonds and MacLennan, 2005). This assumption might not be valid if the fish exhibit diel swimming behaviour. To mitigate this potential problem, others have lowered transducers and a camera closer to the fish targets to: (i) better resolve individuals and (ii) simultaneously assess the species and their orientations (Ona, 2003; Sawada *et al.*, 2009).

The lack of TS values for European anchovy (*Engraulis encrasicolus*) and sardine (*S. Pilchardus*) in the literature has been pointed out by the Working Group on Acoustic and Egg Surveys for Sardine and Anchovy in the Bay of Biscay and Iberican peninsula areas (ICES, 2008). In the Bay of Biscay, dense sound scattering layers (SSL) are observed near the surface at night in springtime. In this case, the TS of small pelagic fish cannot be distinguished from that of other scatterers. Therefore, TS measurements must be made during daytime, within highly packed small pelagic fish schools. We present a method to measure daytime TS of small pelagic fish in their natural environment, while observing the species, its length, and orientation relative to the incident acoustic wave (incident angle). The method involves the use of a pelagic trawl fitted with a codend opening system, "ENROL", to herd and orient fish, and Ifremer's Remotely Operated Towed Vehicle (ROTV), "EROC", to make acoustic measurements and video observations. The method was used to assess the daytime TS of European anchovy (*E. encrasicolus*) in the Bay of Biscay. Reults are compared to published values of clupeiforms mean TS obtained for a range of natural incidence angles and discussed in the light of TS modelling results obtained for *E. encrasicolus.*

Material and methods

The ROTV EROC (Engin Remorqué d'Observation de Chalut) (Figure 1a) was originally used by the Ifremer Research and Technological Development Department for trawl observations. The 2.3-m long, 1.6-m wide and 1.6-m high ROTV weighs 400 kg and is equipped with a stainless steel frame, anodized aluminium rotors, and high density foam floats ensuring positive buoyancy. It is towed behind the vessel at the end of a 21-mm diameter, 1000 m long cable fitted with optic fibre. It can be moved, in real time, in the vertical and horizontal planes using two Magnus effect rotors. Its positive buoyancy housing allows for deployments as deep as 300 m, at speeds from two to four knots, nominally three knots. It is enclosed in a protective cage that ensures safe deployment and retrieval through the stern trawler ramp. The ROTV EROC is equipped with motion and pressure sensors recording roll, pitch and depth values every 2 s, and a black and white, high definition, low-light pan and tilt camera, whose images are displayed in real time for the pilot to locate and manoeuvre the ROTV. The camera outputs can be recorded in real time by a DVD recorder. A split-beam echosounder (Simrad EK60) fitted with a deep water 70-kHz transducer (Transonics) with a nominal 7° beam angle was added to the system. To assess the effect of pressure and temperature variations on the transducer, on-axis calibrations of the echosounder were performed at 10, 30, 55, and 70 m depth using a standard method (Foote *et al.*, 1987), on 30 May 2015.

The echosounder was operated at the highest transmit rate (20 transmissions per second, on an average) and shortest pulse duration (128 μs) available, to provide 30-cm horizontal and 10-cm vertical sampling resolutions.

The codend of the pelagic trawl (two doors, headline = 57 m, foot rope = 52 m) was replaced with a cylindrical frame of neutral buoyancy called the "ENROL" (ENgin Remorqué d'Observation non Léthale, Figure 1b), to allow fish escapement (Figure 4). The

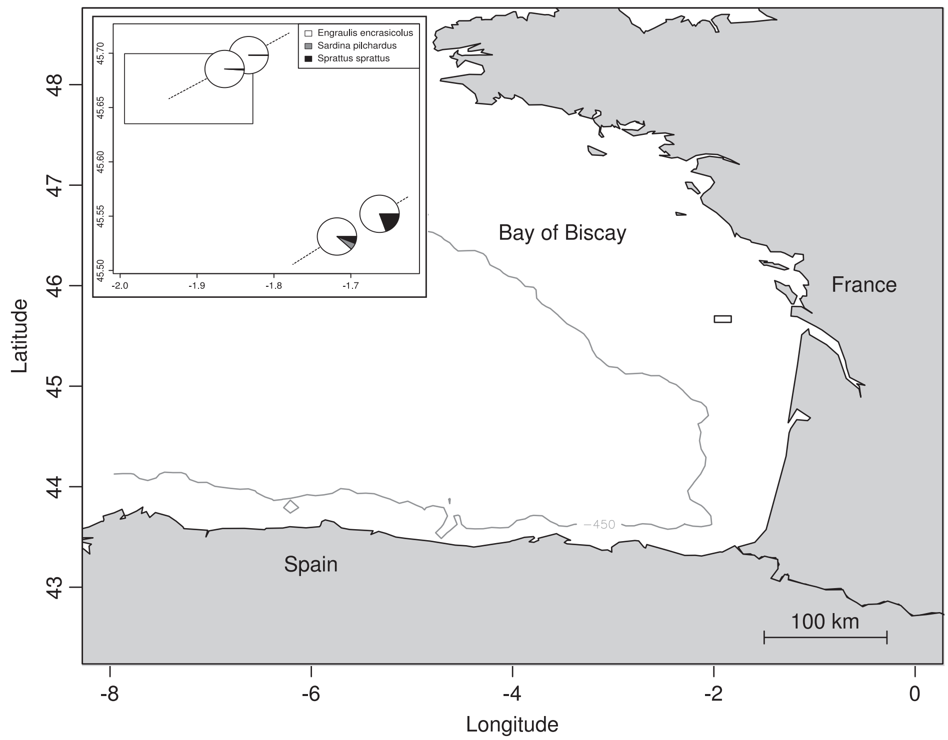

Figure 2. Bay of Biscay map showing the 450-m isobath (continental shelf limits, grey line) and the area where anchovy target strengths (TS) were recorded (black rectangle). The upper-left panel is a zoom on the study area showing the TS recording area (black rectangle), the paths of the four identification trawl hauls (dotted lines), and pie charts presenting the trawl catch relative composition (*Engraulis encrasicolus* in white, *Sardina pilchardus* in grey, and *Sprattus sprattus* in black.

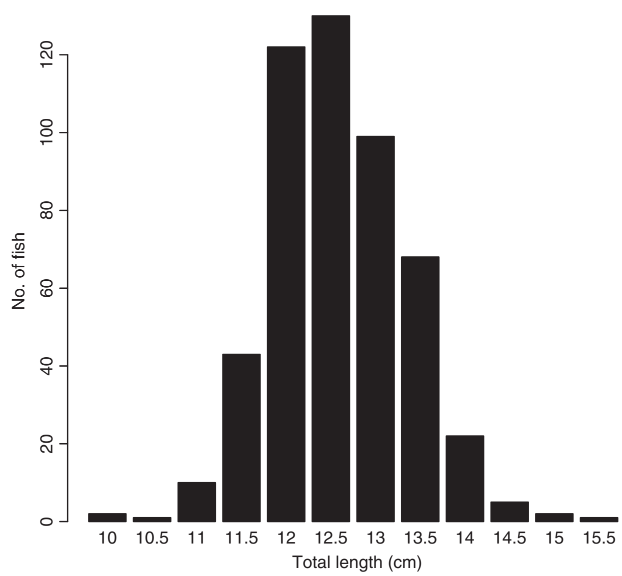

Figure 3. Histogram of the length distribution of *Engraulis encrasicolus* caught in the study area (N=4 trawl hauls, mean anchovy proportion in the catch: 88%).

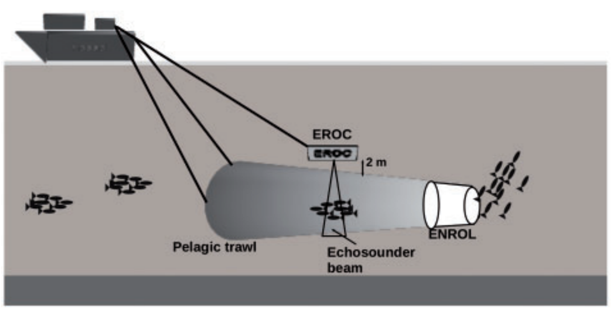

Figure 4. Scheme of the EROC-ENROL target strength recording configuration.

Table 1. Target strength detection parameters.

Parameter	Movies3D	Simrad
Pulse length	0.128 ms	0.128 ms
Min threshold	−60 dB	−60 dB
Min–Max echolength	[0.8–1.8]	[0.8–1.8]
Maximum gain compensation	5 dB	8 dB
Max phase deviation	5	8
Min echo spacing	1	1

objective was to funnel the fish through the open trawl, break up the schools, and allow TS to be measured from dispersed fish swimming in the same direction inside the trawl. As TS were recorded for several hours, the ENROL was configured to allow fish to escape the trawl, to reduce fish mortality during the experiments (Figure 4).

The method can be summarized as follows: (i) during daytime, detect schools of pelagic fish using the vessel's hull-mounted echosounders; confirm the schools are monospecific and identify the species using a midwater trawl; and shoot the ENROL-equipped trawl in the area; (ii) deploy EROC; (iii) locate the trawl using the EROC echosounder, while keeping the ROTV at 10-m depth, to avoid entanglement in the net; (iv) position the EROC 2 m above the central part of the trawl using the camera; (v) record TS of fish attempting to escape the trawl by actively swimming towards the mouth; and (vi) bring EROC closer to the ENROL every hour to observe and identify fish inside the trawl.

The EROC-ENROL method was developed during the PELGAS surveys (Doray *et al*., 2014) in 2011, 2012, 2014 and 2015. The TS measurements presented in this article were made on 31 May 2014 and 1 June 2014, between 10:00 and 18:00 GMT (local time = GMT +2), onboard Ifremer's R/V Thalassa during the PELGAS2014 survey. The system was deployed (N = four trawl hauls) in an area of the Bay of Biscay (mean depth of 64 m) (Figure 2), populated by dense fish school aggregations mostly (mean proportion = 88%) comprised of European Anchovy (mean total length L = 12.5 cm; *SD* = 0.8 cm, Figure 3).

Acoustic data were processed (Movies3D software; Trenkel *et al*., 2009) and archived in the international hydroacoustic data format (HAC; ICES, 2005) with a −80-dB threshold. All single-target echoes with a TS greater or equal to −60 dB were first selected using the EK60 SIMRAD algorithms (Andersen, 2005), implemented with the parameters presented in Table 1. As the number of single echoes selected using this algorithm was low, in comparison to the large number of single targets visible on the echograms, we applied an alternative single-echo detection algorithm (Soule *et al*., 1997), reviewed in ICES (1999), with ad-hoc parameters presented in Table 1 to extract more single echoes. As single echoes were detected in reflections from the trawl head and footropes, as well as from fish, all non-fish TS measurements were removed via visual scrutiny of the TS echogram. The Movies3D target tracking algorithm was applied to the single-fish echoes selected by both algorithms, to derive information on fish swimming behaviour. Refer to appendix 1 for detailed descriptions of the Soule *et al.* (1997) single-echo detection and tracking algorithm implementations in Movies3D. Acceptable tracks had at least 10 detections, no more than one missed observation between consecutive detections, and a maximum speed of five knots (2.57 m s^{-1}). This speed threshold is less than the theoretical maximum burst speed of 6.25 knots (i.e. 25 body length s^{-1}) of a 12.5-cm fish (Wardle, 1975).

The EROC depth was adjusted during the TS recordings, to follow variations in the trawl depth. According to the EROC pressure sensor recordings, the ROTV-depth variations were negligible at the temporal scale of a track (EROC average depth variation during TS recordings: 2 cm, *SD* = 1 cm). The target depth variations during a track were therefore computed based on their positions in the acoustic beam, without correcting for EROC depth variations. The EROC pitch and roll angles were recorded once every 2 s, which is too low compared to the echosounder transmit rate (20 transmissions per second on an average) and the track duration (mean track duration = 1 s) to allow to compute single targets incidence angles by correcting their positions for EROC pitch variations within each transmission or track. In an attempt to assess the uncertainty introduced by the EROC motion in the target orientation estimates, EROC pitch and roll averages and *SD* were computed over all tracks (Table 2). These values being low [EROC average roll during all tracks: 4.1°, *SD* = 1.4°; EROC average pitch during all tracks: 3°, *SD* = 3°)], fish single targets orientations were not corrected for EROC pitch and roll variations.

Table 2. Summary statistics of selected anchovy target strengths data sets.

Data set	1	2	3	4	Average (SD)
Date	05/31/15	05/31/15	06/01/15	06/01/15	
Start time	17:15:00	17:31:17	11:28:42	11:30:14	
End time	17:18:00	17:33:22	11:29:36	11:31:08	
Duration (s)	180	125	54	54	103 (61)
Ping rate (no. Ping.s-1)	20	20	17	17	18 (2)
EROC depth average (*SD*) (m)	49.8 (0.4)	51 (0.3)	55.4 (0.9)	56.1 (0.2)	51.7 (2.6)
EROC depth variation per track (*SD*) (m)	0.008 (0.007)	0.02 (0.01)	0.04 (0.03)	0.03 (0.01)	0.02 (0.01)
EROC roll average (*SD*) (°)	3.6 (1.5)	4.5 (1.6)	2.8 (1.4)	3.9 (0.9)	4.1 (1.4)
EROC pitch average (*SD*) (°)	1.1 (1.0)	0.2 (0.8)	6.3 (2.8)	5.1 (2.4)	3.2 (3)
No. of tracks Movies3D/Simrad	13/6	16/7	25/5	21/10	19 (5)/7 (2)
Total no. of TS in tracks Movies3D/Simrad	186/75	267/143	458/110	364/167	319 (118)/124 (40)
Movies3D/Simrad no. of TS in tracks average (*SD*)	14 (3)/13 (2)	17 (6)/20 (9)	18 (11)/22 (16)	17 (5)/17 (6)	17 (2)/18 (4)
Movies3D/Simrad TS average (5; 95% quantiles) (dB)	−43.7 (−46.3; −41.9)/ −44.1 (−46.7; −41.9)	−43.2 (−45.3; −41.3)/ −43.7 (−47.4; −41)	−43.3 (−46.8; −41.8)/ −44 (−47.7; −42)	−43.1 (−45.9; −41.2)/ −43.3 (−46.3; −41.7)	−43.3 (−46.3; −41.5)/ −43.7 (−47.2; −41.7)
Movies3D global target heading relative vessel heading during track average (*SD*) (°)	−4.7 (4.7)	−7.8 (7.6)	−2.8 (8.3)	−1.9 (7)	−4.3 (2.6)
Movies3D global target pitch angle during track average (*SD*) (°)	−0.2 (0.7)	0 (0.6)	−1 (0.7)	−0.8 (0.5)	−0.5 (0.1)

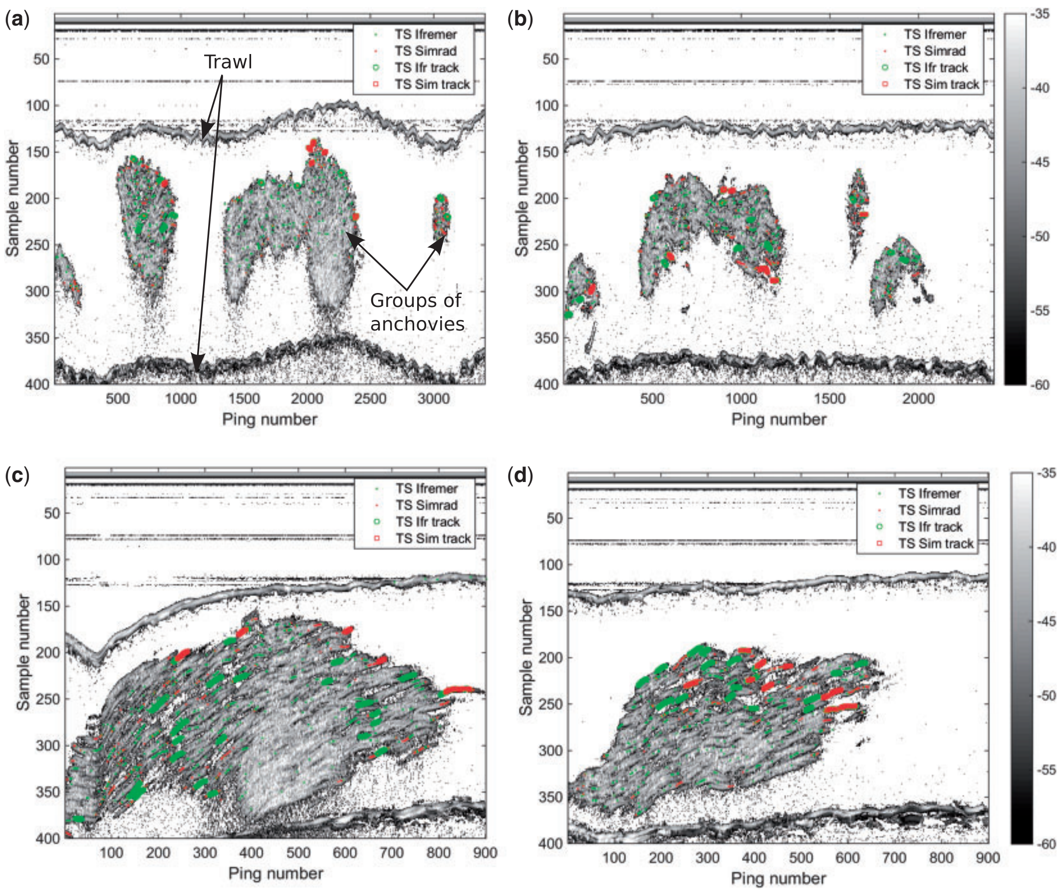

Figure 5. Echograms showing groups of anchovies swimming in a pelagic trawl. Echograms recorded on: (a) 31 May 2015 between 17:15:00 and 17:18:00, (b) 31 May 2015 between 17:31:17 and 17:33:22, (c) 1 June 2015 between 11:28:42 and 11:29:36 and (d) 1 June 2015 between 11:30:14 and 11:31:08. Acoustic densities, expressed as volume backscattering coefficients (S_v in dB), are in grey scale. Small red square dots: single targets detected using Simrad's algorithm, large red empty squares: tracked single targets detected using Simrad's algorithm, small green dots: single targets detected using Movies3D implementation of Soule *et al.* (1997)'s algorithm, large green empty circles: tracked single targets detected using Movies3D implementation of Soule *et al.* (1997)'s algorithm.

The mean target heading of each track, h_{track}, was computed as the average of the i measurements of heading, h_i in the horizontal plane between consecutive target positions in the acoustic beam: $h_i = atan\ (dy_i/dx_i)$, where dx_i is the target displacement to the north, and dy_i is the target displacement to the east (heading north = 0°, anti-clockwise angles). The difference between h_{track} and the vessel heading during the track was used as a proxy for fish heading in the net.

A mean target pitch angle during the track, p_{track}, was computed as the average of the i measurements of pitch p_i in the vertical plane between successive target positions in the acoustic beam: $pitch_i = atan \frac{dz_i}{\left(\sqrt{dx_i^2+dy_i^2}\right)}$, where dx_i is the target displacement to the north, dy_i is the target displacement to the east and dz_i is the target depth variation (horizontal pitch angle = 0°, positive values downwards).

Results

Calibrations results showed a good agreement between the data and the beam model at all depths (mean Root Mean Square, RMS = 0.2 dB, SD = 0.02 dB, see Supplementary Table S4). Significant negative linear relationships were found between the depth covariate and transducer gain, and alongships and athwartships beam angles (see Supplementary Table S4 and Figure S11). No significant relationship was found between the depth covariate and S_a correction. The difference in gain (transducer gain plus S_a correction) between 10 and 70 m was 0.9 dB. This depth-related echosounder gain variation would induce a 1.8 dB difference between TS measurements performed at 10 versus 70 m depth. No relationship was found between the echosounder calibration parameters and the temperature-at-depth.

A total of four acoustic data sets, recorded on 31 May 2014 and 1 June 2014 were selected after single echo detection, tracking, and TS-echogram inspection (Table 2 and Figure 5). As fish TS were recorded between 55- and 60-m depth, the calibration gains obtained at 55 m depth were applied to all targets. Relative to Simrad's single-echo detection algorithm, our implementation of the algorithm proposed by Soule *et al.* (1997), denoted below as 'Movies3D', detected 60% more fish single targets (1287/495), 71% more tracks (76 versus 28), and 160% more tracks per data set (322, SD = 122 versus 124, SD = 40). The tracks derived from both algorithms were of similar length (17, SD = 2 versus 18, SD = 4) (Table 2 and Figure 5).

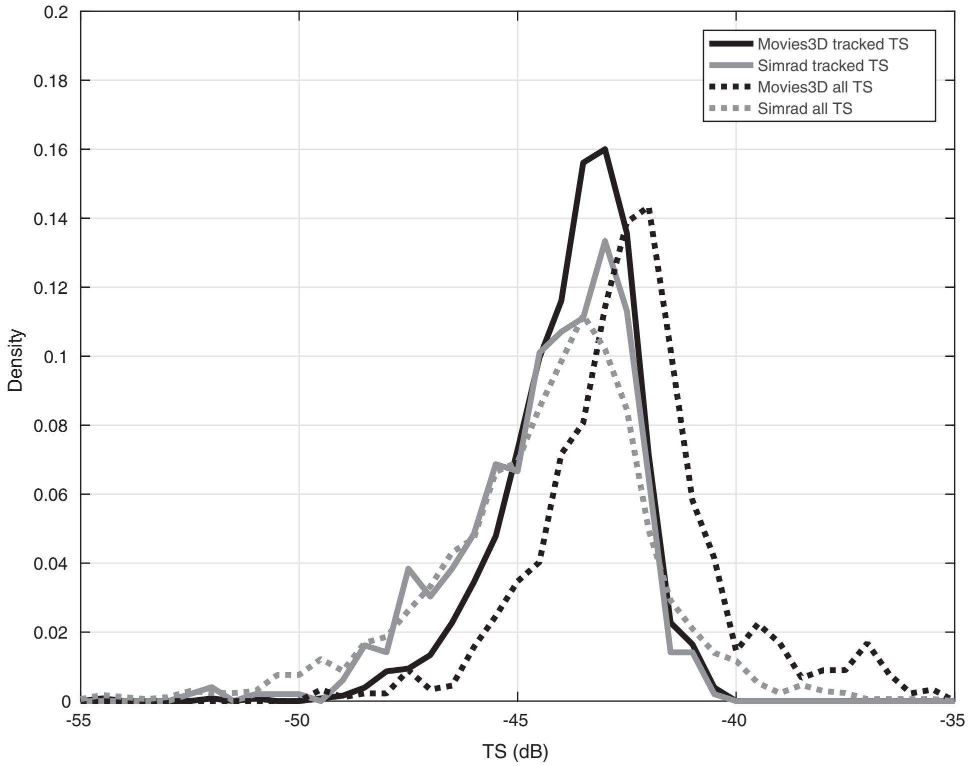

Figure 6. Distributions of *Engraulis encrasicolus* anchovy target strength (TS, in dB) distributions recorded with the EROC-ENROL system. Black solid line: TS distribution after target tracking of single echoes detected using the Movies3D implementation of Soule *et al.* (1997) algorithm. Grey solid line: TS distribution after target tracking of single echoes detected using the Simrad's algorithm. Black dotted line: TS distribution of single echoes detected using the Movies3D implementation of Soule *et al.* (1997) algorithm. Grey dotted line: TS distribution of single echoes detected using Simrad's algorithm.

Fish single targets σ_{bs} [$TS = 10*log10(\sigma_{bs})$]; Simmonds and MacLennan, 2005) were averaged over tracks to filter out the intra-track variability (e.g. incidence angle variations due to fish position in the beam, tilt angle and tail beat effect), then converted to logarithmic TS. The mean TS per track distribution obtained using the Movies3D algorithm over all data sets was nearly symmetrical, centred around the mean = −43.3 dB, with 5% and 95% quantiles equal to −46.3 and −41.5 dB, respectively (Figure 6). The mean TS per track distribution obtained using the Simrad single echo detection algorithm over all data sets was skewed towards low values, with a mean of −43.7 dB and a larger spread (5 and 95% equal to −47.2 and −41.7 dB, respectively (Figure 6). The TS distributions of non-tracked single echoes displayed higher spread, as well as secondary modes (Figure 6). As the Movies3D method provided a higher number of tracked single targets, and therefore more potential information on the fish swimming behaviour in the trawl, as well as a mean TS per track distribution similar to those obtained with the Simrad algorithm, we retained the results derived from the single echoes detected with the Movies3D method for further analysis.

The fish targets global pitch angles during tracks p_{track} were unimodal in all data sets, centered around a mean value = −0.6° (SD = 0.8°) (Figure 7). We then assumed that, apart from EROC pitch and roll, the fish were swimming almost horizontally in the trawl.

Substituting the mean TS and fish total length measurements (L) from this study in the log-linear TS versus L(in cm) relationship: $TS = 20*log_{10}(L)+b_{20}$, the b_{20} value is −65.2 dB.

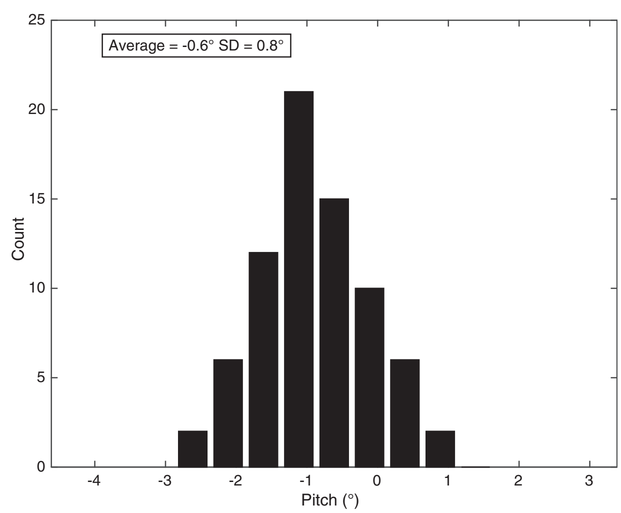

Figure 7. Tracked fish pitch angles estimates. Distribution of fish targets global pitch angles during tracks in all four data sets (mean = −0.6°, SD = 0.8°).

The fish headings in the horizontal plane during tracks relative to EROC heading (p_{track}-heading$_{\mathrm{EROC}}$) were unimodal in all data sets, centred around a mean value = −3.9°, and narrowly spread to the right tail (SD = 7.7°) (Figure 8). This indicates that most of the fish were swimming almost parallel to the trawl. Video

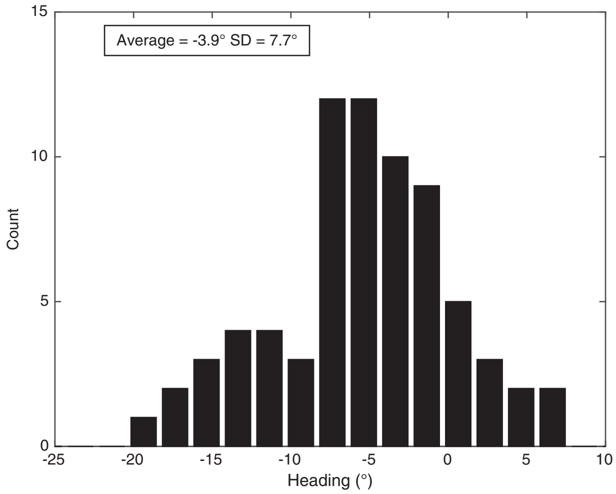

Figure 8. Histogram of the mean heading of anchovies during tracks. Distribution of fish headings in the horizontal plane during tracks, relatively to the vessel heading (0° = vessel heading, fish headings mean average = −3.9°, *SD* = 7.7°).

recording confirmed these results and further demonstrated that the fish were swimming towards the trawl mouth, and were progressively swept by the current towards the open codend. No relationship was found between the mean TS per track and the track parameters (no. of pings, angles, and depth variation) at the scale of the data sets.

All fish species tended to swim upcurrent, towards the mouth of the trawl, even after having escaped the trawl through the open codend. Most fish swam upcurrent until exhaustion, some escaped through the mesh. When fish reached exhaustion, they were washed out throughout the codend. Small pelagic fish showed very strong school fidelity, sometimes swimming outside the trawl alongside with their conspecifics inside the trawl. All small pelagic fish species inside and outside the trawl showed a strong attraction to light, leading sometimes to escapement, when the EROC lights were switched on at close range.

Discussion and conclusion

The EROC ROTV was first deployed alone during daytime at low speed (3.8 knots), in an area with high density of pure anchovy schools, in an attempt to measure anchovy TS inside schools. No fish TS were recorded in the schools in that way, as fish were too densely packed to allow for single fish TS detection. The ENROL open trawl allowed to herd and scatter small pelagic fish inside the net where they could be individually insonified by the EROC echosounder, hence enabling the recording of small pelagic fish TS during daytime. We observed that the school cohesion was disrupted by the strong current inside the trawl, whereas small pelagic fish quickly reformed schools after exiting the trawl through the ENROL device. This suggest that recording TS inside the trawl with the EROC increases the odds of detecting single echoes of schooling small pelagic fish, compared to measurements conducted on densely packed schools entering the trawl with, e.g. the AOS system (Ryan *et al.*, 2009).

Unsuccessful attempts were made to record the TS of a calibration sphere inside the trawl, to assess the effect of the trawl mesh

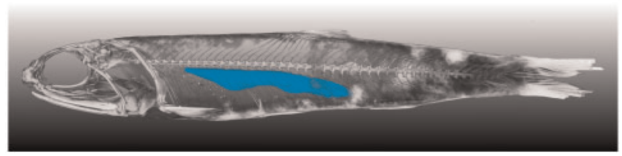

Figure 9. Three-dimensional representation of the swimbladder (blue) and surrounding tissues (greyscale) of a 10.5-cm total length Biscay *Engraulis encrasicolus* specimen, from computed X-ray tomographic imaging.

Table 3. Average and *SD* of the morphological parameters derived from X-ray tomographic (CT) imaging of five *Engraulis encrasicolus* specimen.

Parameter	Value
Fish length average (*SD*) (cm)	10.5 (0.5)
Swimbladder length average (*SD*) (cm)	3 (0.2)
Swimbladder to fish length ratio average (*SD*) (%)	28.3 (1.2)
Swimbladder surface average (*SD*) (cm^2)	2.9 (0.4)
Swimbladder volume average (*SD*) (cm^3)	0.3 (0.06)
Swimbladder equivalent cylinder aspect ratio average (*SD*) (unitless)	10.1 (0.5)
Swimbladder tilt angle average (*SD*) (°)	4.2 (0.9)
Swimbladder equivalent cylinder curvature angle average (*SD*) (°)	10 (3.6)

on TS measurements. We assumed that the effect of the trawl mesh on acoustic measurements was negligible.

The Movies3D implementation of the Soule *et al.* (1997)'s algorithm and Simrad's algorithm are based on the same single target selection principles, but differ in their parameterization. The proposed parameterization allows for the selection of more candidate single targets than Simrad's. The potential multiple targets detected inside the anchovy groups by the Movies3D parameterization of Soule *et al.* (1997)'s algorithm were filtered out during the target tracking step, yielding a higher number of tracked fish single targets than Simrad's algorithm (Table 2 and Figure 5). The use of the proposed single target detection method included more data sets in the analysis that would not have been considered if analysed using the Simrad's algorithm, because of single echoes detection shortage. The higher number of tracked single targets obtained with the Movies3D method also provided: (i) a more symmetrical, unimodal, and narrow distribution of mean TS per track, resulting in a more accurate and precise average TS for anchovy and (ii) more tracks, providing more information on the fish swimming behaviour in the trawl.

Attempts were made to record TS of fish exiting the ENROL at the end of the trawl. These were commonly ∼20 dB lower than the fish TS recorded inside the trawl. Video observations conducted by the EROC near the ENROL, as well as fish depth variations derived from TS tracking suggest that fish exiting the trawl were heavily tilted (∼60°), which likely explains their lower TS values. These low TS values were not retained, as they were not thought to reflect the average, typical, fish swimming behaviour, and could not be distinguished from single targets of other weak scatterers detected around the trawl.

The fish single target positions were not corrected for EROC pitch and roll. As the targets pitch distribution during tracks suggests that fish were on an average swimming almost horizontally,

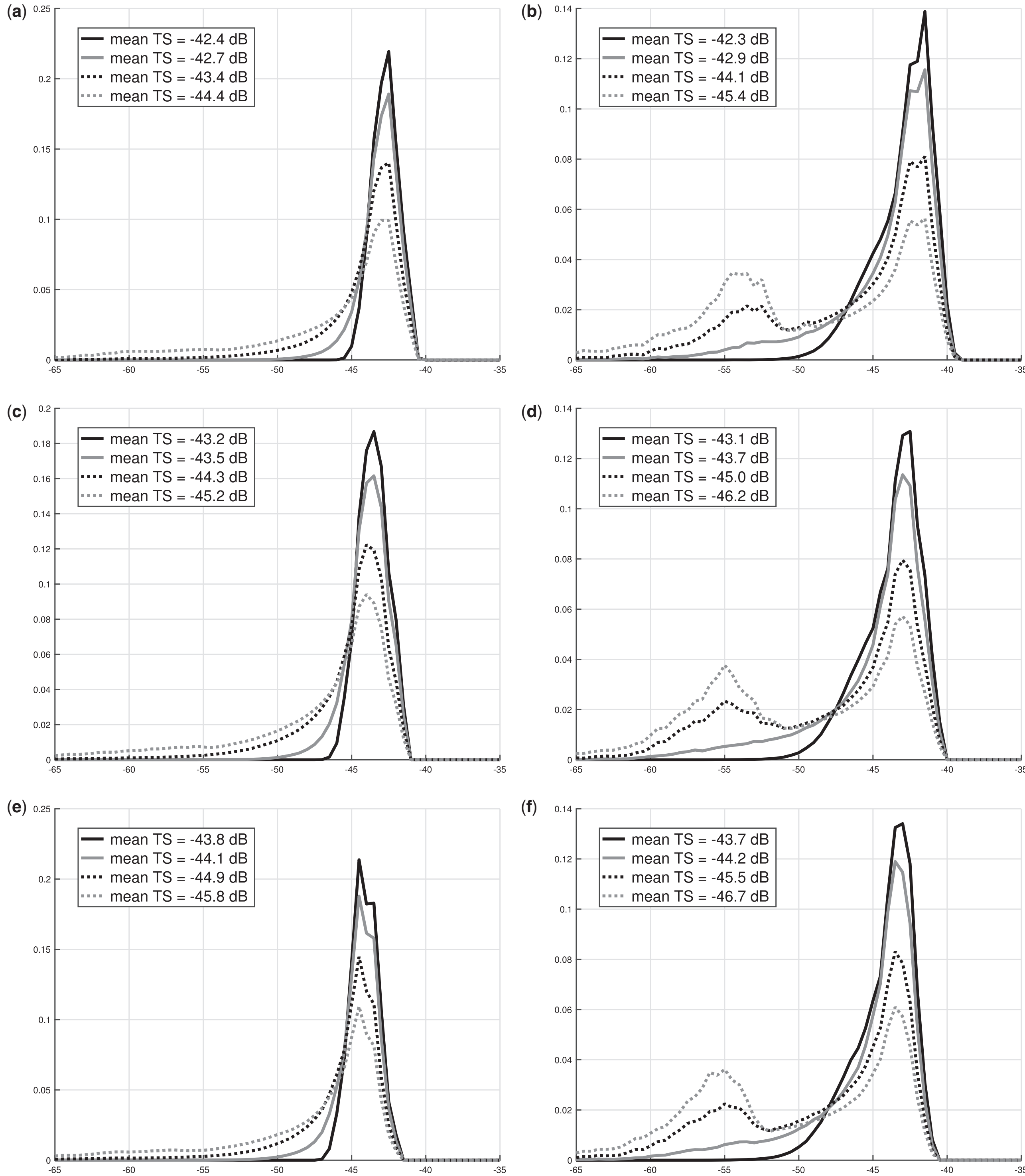

Figure 10. *Engraulis encrasicolus* target strength (TS, in dB) distributions modelled at 38 kHz (a, c, and e) and 70 kHz (b, d, and f) for three swimbladder aspect ratios (a and b: 10, c and d: 15, and e and f: 20) and four fish tilt angle distributions: black solid lines: $N(-0.5°,1)$, grey solid lines: $N(-0.5°,5)$, black dotted lines: $N(-0.5°,10)$, and grey dotted lines $N(-0.5°,15)$.

we instead used the small (<10°, cf. Table 2) EROC pitch and roll variations to further explore the fish acoustic directivity pattern.

This study presents TS values of 12.5 cm *E. encrasicolus* swimming almost horizontally. The mean TS value is 6 dB higher than the theoretical TS predicted for a 12.5-cm *E. encrasicolus* using either the Foote (1987) TS(L) equation for physostomous fish, or the equations used by the French, Spanish and Portuguese research institutes to assess European Anchovy populations biomass (ICES, 2008). Our TS estimate is 2.1 dB higher than those predicted by the Ona (2003) TS(L, depth) equation for a herring swimming at 60-m depth. However, these equations resulted from averages of fish TS measured for a larger range of incidence angles than in our study. TS for fish with a swimbladder is maximum when the maximum swimbladder dimension is perpendicular to the acoustic beam axis, i.e. when the fish swim almost horizontally (Simmonds and MacLennan, 2005). In this article, the anchovy measured using the EROC-ENROL method were swimming almost horizontally, with a low tilt angle *SD*, which is not representative of their natural behaviour. The mean TS value presented in this article was hence computed in a narrow area of the fish directivity pattern, near its maximum. This likely explains why the *E. encrasicolus* TS value derived using the EROC-ENROL method is largely higher than the theoretical values predicted using models established over a wider fish tilt angle distribution.

In a attempt to corroborate our TS measurements, a model of acoustic scattering by *E. Encrasicolus* was developed to investigate the effect of incidence angle and swimbladder compression on fish TS. The swimbladder accounting for 90% or more of the fish acoustic scattering (Foote, 1980), the other organs contribution to total backscatter was neglected. Three-dimensional (3D) representations of the swimbladders were derived from 3D computed X-ray tomographic (CT) imaging. *E. encrasicolus* specimen were collected in the Bay of Biscay and stocked in a 1.5-m deep tank at Aquarium La Rochelle for 7 months. A total of 33 fish were anaesthetized using eugenol for 10–15 min and immediately frozen in liquid nitrogen, to avoid postmortem gas release from the swimbladder. Five suitable specimen (mean total length = 10.5 cm, *SD* = 0.5 cm) were selected after X-ray examination to ensure that the swimbladders were intact and inflated. The five *E. encrasicolus* were examined frozen with Subatech's RX Solutions EasyTom XL 150 X-ray CT scanner. The high image contrast between the gas-filled swimbladder and surrounding organs enabled the precise assessment of the swimbladder boundaries from the CT images (Figure 9). 3D representations of the swimbladders and surrounding tissues were built with the MeVisLab software, using the thresholding method (Figure 9). Key positional and morphological features were derived from swimbladders 3D representations of each anchovy. Swimbladder descriptors means and *SD* (Table 3) were used to parameterize a modal series based deformed cylinder acoustic scattering model (Stanton, 1988, 1989), offset by the average swimbladder tilt angle in the fish (4.2°, *SD* = 0.9°). The model was applied to virtual anchovies randomly distributed in the equivalent aperture of the measured anchovies targets (11°), to derive TS distributions for several frequency:fish tilt angle:swimbladder aspect ratios combinations. TS were predicted for each virtual anchovy as a function of total length, scaled to the observed anchovies length [$L \sim N(12.5, 0.5)$], frequency (38 and 70 kHz) and over tilt angles taken in four normal distributions of identical mean and increasing *SD*: $N(-0.5°,1)$, $N(-0.5°,5)$, $N(-0.5°,10)$ and $N(-0.5°,15)$. The later tilt angle distribution corresponds to various "natural" tilt angle distributions previously measured and used for pelagic species (McClatchie *et al.*, 1996; Faessler *et al.*, 2013). Changes of swimbladder morphology with pressure were simulated by using three different mean aspect ratio: 10 (fully inflated), 15 (partially deflated), and 20 (deflated). TS were predicted for 100 virtual anchovy for each frequency:fish tilt angle:swimbladder aspect ratio combination. The fish length ratio, swimbladder tilt angle and swimbladder curvature values were randomly taken from normal distributions with means and *SD*s equal to those of the average 3D swimbladder representation (Table 3).

The TS distributions obtained at the 38 and 70 kHz frequencies with the three swimbladder aspect ratios and four pitch angle distributions are presented in Figure 10. Modelled mean TS values (computed in the linear domain and converted into logarithmic TS) are very close at the 38 and 70 kHz frequencies for fish tilt angle distribution *SD*s equal to 1° and 5°, and rapidly diverge when the fish tilt angle variance increases. Modelled and observed TS distributions show similar shape, mean and spread at the 70-kHz frequency in the case of virtual fish swimming almost horizontally [fish tilt angle distribution $\sim N(-0.5, 1)$], with swimbladder aspect ratios ranging from 15 to 20 (i.e. for swimbladder compression factors ranging from 1.5 to 2). This compression factor range is less than expected for a free-balloon model, according to Boyle's law (2.6 at 60 m depth). Zhao *et al.* (2008)'s TS measurements of Japanese Anchovy (*E. japonicus*) suggest that the TS depth-dependence of this species might follow Boyle's law. Their study was however based on a relatively small sample, collected within a narrow (20–40 m) and more shallow depth layer than in our study, and without information on fish tilt angles. On the other hand, Ona (2003)'s empirical TS(L,depth) equation based on extensive TS measurements at depths down to 500 m predicts a compression factor (1.56) within the range of our modelling results, for a 12.5-cm herring (*Clupea harengus*) swimming at 60-m depth. Moreover, our modelling results show that an increase of the fish tilt angle distribution *SD* from 1° (near horizontal swimming behaviour) to 15° ("natural" swimming pattern) leads to a 2- to 3-dB decrease of the mean TS values, at the 38 and 70 kHz frequencies, respectively. Updating the log-linear TS versus length relationship for *E. encrasicolus* with the 2-dB decrease predicted at 38 kHz yields a b_{20} values of −63.2 dB. This value is in line with the TS predicted at the 38-kHz frequency by the Ona (2003) TS(L, depth) equation for a 12.5-cm herring swimming at 60 m depth. Assuming that the *E. encrasicolus* swimbladder compression factor at 60 m depth lies in the wild between 1.5 and 2, which seems likely according to Ona (2003)'s study on herring, our modelling results confirm that the measured TS value presented in this article is a realistic estimate of the maximum TS of a 12.5-cm *E. encrasicolus* at 60-m depth, that could be used to scale and evaluate future TS models for this species.

Complementary modelling and *ex situ* experiments should be conducted to derive robust TS(L, depth) equations that account for the natural tilt angle distribution of *E. encrasicolus*. The use of a pan and tilt transducer on the EROC would facilitate sampling of TS over a large range of incidence angles and at different depths.

In summary, the EROC/ENROL method can be used to measure TS of small pelagic fish while controlling for species, length, and incidence angle. Repeated EROC/ENROL-based TS measurements on monospecific schools should result in accurate TS(L) equations for small pelagic fish species, near normal incidence.

Supplementary data

Supplementary material is available at the *ICESJMS* online version of the manuscript.

Acknowledgements

We thank the Thalassa crew for their invaluable assistance in designing, building and operating the ENROL open trawl. The TS modelling work was funded by the Ifremer's "Politique de site" project TOMOFISH. We thank Dr Carla Scalabrin for initial development and testing of the acoustic payload of the EROC ROTV. We acknowledge the two referees and the editor for their useful comments that helped improving the article. Special thanks to Dr Marie Laure Nauleau for her patience.

References

Andersen, L. 2005. Status and plans for the ER60/EK60. ICES WGFAST Report, 2005/B:05: 20.

Balk, H., Lindem, T. 2003. Sonar5–Pro, post processing system. Operator manual. http://folk.uio.no/hbalk/exchange_files/Manual_SonarX%20v601%20for%20printing_28_03_2012.pdf.

Barange, M. 1994. Acoustic identification, classification and structure of biological patchiness on the edge of the Agulhas Bank and its relation to frontal features. South African Journal of Marine Science, 14: 333–347.

Barange, M., Hampton, I., and Soule, M. 1996. Empirical determination of target strengths of three loosely aggregated pelagic fish species. ICES Journal of Marine Science, 53: 225–232.

Doray, M., Badts, V., Massé, J., Duhamel, E., Huret, M., Doremus, G., and Petitgas, P. 2014. Manual of fisheries survey protocols. PELGAS surveys (PELagiquesGAScogne). Manuel des protocoles de campagne halieutique Ifremer, 30259. http://archimer.ifremer.fr/doc/00191/30259/28714.pdf.

Doray, M., Josse, E., Gervain, P., Reynal, L., and Chantrel, J. 2006. Acoustic characterisation of pelagic fish aggregations around moored fish aggregating devices in Martinique (Lesser Antilles). Fisheries Research, 82: 162–175.

Doray, M., Josse, E., Gervain, P., Reynal, L., and Chantrel, J. 2007. Joint use of echosounding, fishing and video techniques to assess the structure of fish aggregations around moored Fish Aggregating Devices in Martinique (Lesser Antilles). Aquatic Living Resources, 20: 357–366.

Faessler, S. M. M., O'Donnell, C., and Jech, J. M. 2013. Boarfish (Capros aper) target strength modelled from magnetic resonance imaging (MRI) scans of its swimbladder. ICES Journal of Marine Science, 70: 1451–1459.

Foote, K. G. 1980. Importance of the swimbladder in acoustic scattering by fish: a comparison of gadoid and mackerel target strengths. Journal of Acoustical Society of America, 67: 2084–2089.

Foote, K. G. 1987. Fish target strengths for use in echo integrator surveys. Journal of Acoustical Society of America, 82: 981–987.

Foote, K. G., Knudsen, H. P., Vestnes, G., MacLennan, D. N., and Simmonds, E. J. 1987. Calibration of acoustic instruments for fish density estimation: a practical guide. ICES Cooperative Research Report, 144: 57.

Fréon, P., and Misund, O. A. 1999. Dynamics of Pelagic Fish Distribution and Behaviour: Effects on Fisheries and Stock Assessment. Blackwell, Oxford.

Horne, J. K. 2000. Acoustic approaches to remote-species identification: a review. Fisheries Oceanography, 9: 356–371.

ICES. 1999. Method for target strength measurements. ICES Cooperative Research Report, 235: 59.

ICES. 2005. Description of the ICES HAC standard data exchange format, version 1.60. ICES Cooperative Research Report, 278: 86.

ICES. 2008. Report of the Working Group on Acoustic and Egg Surveys for Sardine and Anchovy in ICES Areas VIII and IX (WGACEGG). ICES CM, 2008/LRC:17. 183 pp.

Jech, J., and Horne, J. K. 2001. Effects of in situ target spatial distributions on acoustic density estimates. ICES Journal of Marine Science, 58: 123–136.

Kubilius, R., and Ona, E. 2012. Target strength and tilt-angle distribution of the lesser sandeel (*Ammodytes marinus*). ICES Journal of Marine Science, 69: 1099–1107.

McClatchie, S., Alsop, J., and Coombs, R. F. 1996. A re-evaluation of relationships between fish size, acoustic frequency, and target strength. ICES Journal of Marine Science, 53: 780–791.

O'Driscoll, R. L., Oeffner, J., and Dunford, A. J. 2013. In situ target strength estimates of optically verified southern blue whiting (*Micromesistius australis*). ICES Journal of Marine Science, 70: 431–439.

Ona, E. 2003. An expanded target-strength relationship for herring. ICES Journal of Marine Science, 60: 493–499.

Peltonen, H., and Balk, H. 2005. The acoustic target strength of herring (*Clupea harengus* L.) in the northern Baltic Sea. ICES Journal of Marine Science, 62: 803–808.

Rose, G. 1992. A review of problems and new directions in the application of fisheries acoustics on the Canadian east coast. Fisheries Research, 14: 105–128.

Ryan, T. E., Kloser, R. J. and Macaulay, G. J. 2009. Measurement and visual verification of fish target strength using an acoustic-optical system attached to a trawlnet. ICES Journal of Marine Science, 66: 1238–1244.

Sawada, K., Takahashi, H., Abe, K., Ichii, T., Watanabe, K., and Takao, Y. 2009. Target-strength, length, and tilt-angle measurements of Pacific saury (*Cololabis saira*) and Japanese anchovy (*Engraulis japonicus*) using an acoustic-optical system. ICES Journal of Marine Science, 66: 1212–1218.

Simmonds, E. J., and MacLennan, D. N. 2005. Fisheries Acoustics. Theory and Practice. Blackwell Publishing, Oxford. 456 pp.

Soule, M., Barange, M., and Hampton, I. 1995. Evidence of bias in estimates of target strength obtained with a split-beam echo-sounder. ICES Journal of Marine Science, 52: 139–144.

Soule, M., Barange, M., Solli, H., and Hampton, I. 1997. Performance of a new phase algorithm for discriminating between single and overlapping echoes in a split-beam echosounder. ICES Journal of Marine Science, 54: 934–938.

Stanton, T. K. 1988. Sound scattering by cylinder of finite length. I. Fluid cylinders. Journal of the Acoustical Society of America, 83: 55–63.

Stanton, T. K. 1989. Sound scattering by cylinder of finite length. III. Deformed cylinders. Journal of the Acoustical Society of America, 86: 691–705.

Trenkel, V. M., Berger, L., Bourguignon, S., Doray, M., Fablet, R., Massé, J., and Villalobos, H. 2009. Overview of recent progress in fisheries acoustics made by Ifremer with examples from the Bay of Biscay. Aquatic Living Resources, 22: 433–445.

Wardle, C. S. 1975. Limit of fish swimming speed. Nature, 255: 725–727.

Zhao, X., Wang, Y., and Dai, F. 2008. Depth-dependent target strength of anchovy (*Engraulis japonicus*) measured in situ. ICES Journal of Marine Science, 65: 882–888.

Handling editor: David Demer

Appendix 1

Single echo detection and tracking method

Our Matlab implementation of the Soule *et al.* (1997) algorithm is similar to those used in other acoustic data post-processing systems (e.g. EK60, Andersen 2005, Echoview, www.echoview.com, Sonar5, Balk and Linderm 2003). Based on S_v, alongships and athwartships phase angles values stored in HAC files, target strength (TS) compensated (TS_{comp}) or uncompensated (TS_{uncomp}) for beam pattern are computed, as well as TS_{uncomp}values uncompensated for transmission losses (P_{like}), derived as: $P_{like}= TS_{uncomp}-40logR-2.\alpha.R$, where α is the absorption coefficient and R the range to the transducer. The beam pattern compensation is computed using the Simrad's small angle approximation for a weighted transducer as: $TS = TS_{uncomp}+ 6.0206*(x^2 + y^2-0.18*x^2.*y^2)$, with $x = 2.(al\text{-}ofs_{al})/\Theta_{al}$ and $y = 2.(at\text{-}ofs_{at})/\Theta_{at}$, where al and at are the alongships and athwartships angles, ofs_{al} and ofs_{at} are the alongship and athwartship calibrated steering offsets, and Θ_{al} and Θ_{at} are the alongships and athwartships one-way 3-dB beamwidths.

The single targets detection method comprises the following steps, illustrated in Supplementary Figure S12:

(1) Selecting initial single echoes candidates as: (i) echoes whose P_{like} value is a local maximum ($P_{like\text{-}max}$) and (ii) echoes whose TS values are higher than a user defined threshold.

(2) Filtering based on echo length. The echo length is defined as the number of samples before and after $P_{like\text{-}max}$, for which P_{like} values are higher than $P_{like\text{-}max}$-6 dB. The echo is retained if its length falls between user defined, minimum and a maximum normalized pulse length values.

(3) Filtering based on maximum beam compensation values, computed as: $TS_{comp}-TS_{uncomp}$. Echoes with maximum beam compensations lesser than a user-defined threshold are retained.

(4) Filtering based on phase angles, to filter out echoes that are not angularly coherent over a pulse duration, defined as five consecutive samples around $P_{like\text{-}max}$. Echoes whose alongships and athwartships phase angles *SD*s are lower than a used-defined threshold are retained.

(5) Filtering based on distance to stronger neighbouring echo. A fine scale range is computed for each retained local maxima, as the average of the $P_{like\text{-}max}$ samples ranges, weighted by the P_{like} sample values over the echo length. An accurate transmission loss compensation is computed for each echo, based on their fine scale range. Echoes are finally retained if their distance to the nearest echo displaying a stronger $P_{like\text{-}max}$ is higher than a user defined threshold.

The retained single echoes are then tracked, using the following method, illustrated in Supplementary Figure S13:

(1) Single echoes positioning and track initialization. The positions of all single targets are computed in a geographic coordinate system defined by an origin at the position where data acquisition started, an *x*-axis in the horizontal plane, with positive values to the North, a *y*-axis in the horizontal plane, with positive values to the East, and a *z*-axis with positive values downwards. Each single echo is initially considered as a track.

(2) Distance-based target tracking. The following target tracking procedure is iteratively applied on all pings, starting at ping number $N = 1$. Assuming that the EROC follows the vessel track at the same speed, the distances between each single target in ping $N + 1$ and all single echoes in ping N are computed, based on inter-ping times, target ranges and vessel speed. A single echo s_{N+1} in ping $N + 1$ is assigned to the track comprising the single echo s_N in ping N if the distance between s_N and s_{N+1} is smaller than a user-defined maximum displacement between two consecutive pings, and if s_N is the closest single echo to s_{N+1}. If no single echo s_N satisfies these conditions, computations in step 2 are performed on single targets in pings $N + 1$ and $N-1$, allowing for a 1-echo gap between two consecutive targets in the tracks. If ping $N-1$ does not exist, or if no single echo satisfying the conditions is found in ping $N-1$, s_{N+1} is associated to no single echo in previous pings.

(3) Track length and wholeness filtering. Tracks with a number of single echoes and a relative number of gaps, respectively, higher and lesser than user-defined thresholds are actually retained.